



Evidence for $B^+ \rightarrow \omega l^+ \nu$

C. Schwanda* (for the Belle collaboration)

High Energy Accelerator Research Organization (KEK), Tsukuba, Japan

We have searched for the decay $B^+ \rightarrow \omega l^+ \nu$ in 78 fb⁻¹ of $\Upsilon(4S)$ data (85.0 million $B\bar{B}$ events) accumulated with the Belle detector. The final state is fully reconstructed using the ω decay into $\pi^+\pi^-\pi^0$ and the detector hermeticity to infer the neutrino momentum. The signal yield is extracted by a two-dimensional fit to the lepton momentum and the invariant $\pi^+\pi^-\pi^0$ mass. The result of the fit depends on the form factor model assumed for the decay. Taking the average over three different models, 421 ± 132 events are found in the data, corresponding to a preliminary branching fraction of $(1.4 \pm 0.4(stat) \pm 0.2(syst) \pm 0.3(model)) \cdot 10^{-4}$.

1 Introduction

Tree-level semileptonic B decays are crucial for measuring the CKM matrix elements $|V_{cb}|$ and $|V_{ub}|$ [1] independently of any new physics contribution. The decay $B \rightarrow X_u l \nu$ ¹ (which allows to access $|V_{ub}|$) has been studied both using inclusive approaches (sensitive to all $X_u l \nu$ final states within a given region of phase space) and through exclusive reconstruction of specific final states [2]. As to the latter, Belle has already obtained preliminary results for the decays $B^0 \rightarrow \pi^- l^+ \nu$ and $B^+ \rightarrow \rho^0 l^+ \nu$ [3]. In this article, we present evidence for the decay $B^+ \rightarrow \omega l^+ \nu$ which is so far unobserved.

2 Experimental procedure

2.1 KEKB and the Belle detector

Belle is located at the KEKB asymmetric e^+e^- collider, operating at the $\Upsilon(4S)$ resonance [4]. The detector is described in detail elsewhere [5]. It is a large-solid-angle magnetic spectrometer that consists of a three-layer silicon vertex detector (SVD), a 50-layer central drift chamber (CDC), an array of aerogel threshold Čerenkov counters (ACC), a barrel-like arrangement of time-of-flight scintillation counters (TOF), and an electromagnetic calorimeter comprised of CsI(Tl) crystals (ECL) located inside a superconducting solenoid coil that provides a 1.5 T magnetic field.

The responses of the ECL, CDC (dE/dx) and ACC detectors are combined to provide clean electron identification. Muons are identified in the instrumented iron flux-return (KLM) located outside of the coil.

Charged hadron identification relies on information from the CDC, ACC and TOF.

2.2 The data set

This analysis is based on an integrated luminosity of 78.13 fb⁻¹ taken on the $\Upsilon(4S)$ resonance. This data set contains $(85.0 \pm 0.5) \cdot 10^6$ $B\bar{B}$ events. Furthermore, to subtract the hadronic background, 8.83 fb⁻¹ taken below the resonance are used.

Full detector simulation is applied to Monte Carlo events. Generic background Monte Carlo samples, equivalent to about three times the beam luminosity, are used in various stages of this analysis. Monte Carlo samples for the signal, $B^+ \rightarrow \omega l^+ \nu$, are generated with the following form factor models: ISGW2 (quark model [6]), UKQCD (quenched lattice QCD calculation [7]) and LCSR (light cone sum rules [8]). The cross-feed from other decays $B \rightarrow X_u l \nu$ is estimated using the ISGW2 Monte Carlo.

2.3 Neutrino reconstruction

Events passing the hadronic selection are required to contain a single lepton (electron or muon) with a c.m. momentum p_i^* greater than 1.3 GeV/ c . In this momentum range, electrons (muons) are selected with an efficiency of 92% (89%) and a pion fake rate of 0.25% (1.4%). This requirement is 41% efficient for $B \rightarrow X_u l \nu$ events.

The missing four-momentum is computed for selected events,

$$\begin{aligned} \vec{p}_{miss} &= \vec{p}_{HER} + \vec{p}_{LER} - \sum_i \vec{p}_i, \\ E_{miss} &= E_{HER} + E_{LER} - \sum_i E_i, \end{aligned} \quad (1)$$

where the sum runs over all reconstructed charged tracks and photons. The indices HER and LER re-

*Supported by the Japan Society for the Promotion of Science.
¹Throughout this article, the inclusion of the charge conjugate mode is implied.

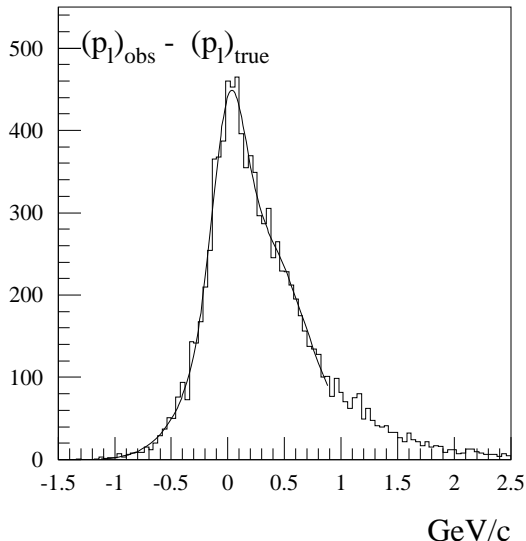


Figure 1. The missing momentum resolution in $B \rightarrow X_u l \nu$ events (ISGW2 model). The fit shown uses a double Gaussian ($\sigma_1 = 141 \pm 10$ MeV/c, $\sigma_2 = 412 \pm 8$ MeV/c).

fer to the high energy and the low energy ring, respectively. To reject events in which the missing momentum does not match the neutrino momentum, the following selection criteria are applied. Events with a large charge imbalance are eliminated, $|Q_{tot}| < 3e$, and the direction of the missing momentum is required to lie within the ECL acceptance, $17^\circ < \theta_{miss} < 150^\circ$. The missing mass squared, $m_{miss}^2 = E_{miss}^2 - \vec{p}_{miss}^2$, is required to be consistent with the neutrino hypothesis, $|m_{miss}^2| < 3 \text{ GeV}^2/c^4$.

After applying these cuts, the resolution in p_{miss} (E_{miss}) is found to be 141 MeV/c (587 MeV) for simulated $B \rightarrow X_u l \nu$ events (Fig. 1). As the energy resolution is worse than the momentum resolution, the neutrino four-momentum is taken to be $(p_{miss}, \vec{p}_{miss})$. The efficiency of the event selection and neutrino reconstruction cuts is about 17% for $B \rightarrow X_u l \nu$ events.

2.4 Final state reconstruction

Pairs of γ 's are combined to form π^0 candidates ($E_\gamma > 30$ MeV, $120 < m(\gamma\gamma) < 150$ MeV/c²). The decay $\omega \rightarrow \pi^+\pi^-\pi^0$ (branching ratio: $(89.1 \pm 0.7)\%$ [9]) is reconstructed by trying all possible combinations of one π^0 with two oppositely charged tracks. Combinations with a charged track identified as a kaon are rejected and the following selections are imposed: $p_\omega^* > 300$ MeV/c, $703 < m(\pi^+\pi^-\pi^0) < 863$ MeV/c². Combinations located far away from the center of the Dalitz plot are removed by requiring the Dalitz amplitude, $A \propto |\vec{p}_{\pi^+} \times \vec{p}_{\pi^-}|$, to be larger than half of its

maximum value.

The single lepton in the event is combined with the ω candidate and the inclusive neutrino, and the lepton momentum cut is tightened, $1.5 < p_l^* < 2.7$ GeV/c. To reject combinations inconsistent with signal decay kinematics, the cut $|\cos\theta_{BY}| < 1.1$ is imposed,

$$\cos\theta_{BY} = \frac{2E_B^*E_Y^* - m_B^2 - m_Y^2}{2p_B^*p_Y^*}, \quad (2)$$

where E_B^* , p_B^* and m_B are fixed to their nominal values, $\sqrt{E_{HER}E_{LER}}$, $\sqrt{E_B^{*2} - m_B^2}$ and 5.279 GeV/c², respectively. E_Y^* , p_Y^* and m_Y are the measured c.m. energy, momentum and mass of the $Y = \omega + l$ system, respectively. For well-reconstructed signal events, $\cos\theta_{BY}$ is the cosine of the angle between the B and the Y system and lies between -1 and $+1$ while for the various backgrounds, a significant fraction is outside this interval.

For each $\omega l \nu$ candidate, the beam-constrained mass m_{bc} and ΔE are calculated ($E_{beam}^* = \sqrt{E_{HER}E_{LER}}$),

$$m_{bc} = \sqrt{(E_{beam}^*)^2 - |\vec{p}_\omega^* + \vec{p}_l^* + \vec{p}_\nu^*|^2}, \quad (3)$$

$$\Delta E = E_{beam}^* - (E_\omega^* + E_l^* + E_\nu^*),$$

and candidates in the window $m_{bc} > 5.23$ GeV/c² and $|\Delta E| < 0.36$ GeV are selected. On the average, two combinations per event remain after applying all cuts. We choose the one with the largest ω momentum in the c.m. frame, which is the right choice about 80% of the time.

2.5 Continuum suppression

The hadronic continuum from $e^+e^- \rightarrow q\bar{q}$ events, $q = u, d, s, c$, is suppressed using three variables exploiting the fact that, in the $\Upsilon(4S)$ frame, the two B mesons are produced nearly at rest and that therefore $B\bar{B}$ events have a nearly spherical shape while continuum events have a more jet-like topology. These variables are:

- The ratio R_2 of the second to the zeroth Fox-Wolfram moment [10]. This ratio tends to be close to zero (unity) for spherical (jet-like) events. (The cut $R_2 < 0.4$ is imposed already at the event selection level.)
- The cosine of θ_{thrust} , where θ_{thrust} is the angle between the thrust axis of the ωl system and the thrust axis of the rest of the event.
- A Fisher discriminant selecting events with an even energy distribution around the lepton direction [11]. The input variables are the charged and neutral energy in nine cones of equal solid angle around the lepton momentum axis.

To optimize their individual discriminating power, these three variables are combined into a likelihood ratio. This selection is 55% efficient for $B^+ \rightarrow \omega l^+ \nu$ events, while 92% of the continuum background remaining after the $R_2 < 0.4$ cut, is eliminated.

2.6 The fit

The amount of signal and the remaining background in the m_{bc} vs. ΔE signal window are determined by a two-dimensional binned likelihood fit to the lepton momentum p_l^* (4 bins, width: 300 MeV/c) and the invariant mass $m(\pi^+ \pi^- \pi^0)$ (8 bins, width: 20 MeV/c²) [12]. The following five components are fitted to the data: $B^+ \rightarrow \omega l^+ \nu$ signal, $B \rightarrow X_u l \nu$ background, $B \rightarrow X_c l \nu$ background, fake and non B decay lepton background and continuum. The shapes of the former four components are determined from the simulation, the shape of the continuum component is given by the off-resonance data. The normalizations of the $B^+ \rightarrow \omega l^+ \nu$, the $B \rightarrow X_u l \nu$ and the $B \rightarrow X_c l \nu$ component are floated in the fit, the other components being fixed (Fig. 2).

3 Result and systematic uncertainty

The signal yield, $N(B^+ \rightarrow \omega l^+ \nu)$, is determined separately for each form factor model and the branching ratio, $\mathcal{B}(B^+ \rightarrow \omega l^+ \nu)$, is calculated using the relation

$$N(B^+ \rightarrow \omega l^+ \nu) = N(B^+) \times \mathcal{B}(B^+ \rightarrow \omega l^+ \nu) \times \mathcal{B}(\omega \rightarrow \pi^+ \pi^- \pi^0) \times (\epsilon_e + \epsilon_\mu), \quad (4)$$

where $N(B^+)$ is the total number of charged B mesons in the data, $\mathcal{B}(\omega \rightarrow \pi^+ \pi^- \pi^0) = (89.1 \pm 0.7)\%$ [9] and ϵ_e (ϵ_μ) is the model dependent selection efficiency for the electron (muon) channel (Table 1). Averaging over the three models (giving equal weight to each), 421 ± 132 signal events are found in the data, corresponding to a branching fraction of $(1.4 \pm 0.4(stat)) \cdot 10^{-4}$. The spread between the different models amounts to 21% and is used as an estimate of the form factor model uncertainty.

The largest experimental uncertainty is the efficiency of the neutrino reconstruction (7.5%). It is estimated by varying the track finding efficiency, the neutral cluster finding efficiency, the track momentum resolution and the cluster energy resolution separately in the Monte Carlo within their estimated range of uncertainty. The next to largest component is the cross-feed from decays $B \rightarrow X_u l \nu$ (4.4%) which is estimated by varying the fraction of $B \rightarrow \pi l \nu$ and $B \rightarrow \rho l \nu$ (these decays are expected to dominate in the high p_l^* region) within their experimental uncertainty. Other contributions are: $B \rightarrow X_c l \nu$ cross-feed

(2.4%), charged track and cluster finding (3.0% and 4.0%, respectively), lepton identification (3.0%), the number of $B\bar{B}$ events (0.6%) and the uncertainty in the $\omega \rightarrow \pi^+ \pi^- \pi^0$ branching fraction (0.8%).

4 Conclusion

We have measured the decay $B^+ \rightarrow \omega l^+ \nu$ using 78 fb^{-1} of $\Upsilon(4S)$ data (85.0 million $B\bar{B}$ events). The final state of the decay was fully reconstructed using the ω decay into $\pi^+ \pi^- \pi^0$ and detector hermeticity to infer the neutrino momentum. The signal yield was determined by a two-dimensional fit to the lepton momentum and the invariant $\pi^+ \pi^- \pi^0$ mass. Repeating the fit for three different $B^+ \rightarrow \omega l^+ \nu$ form factor models and averaging the result, 421 ± 132 signal events are found, corresponding to a branching fraction of $(1.4 \pm 0.4(stat) \pm 0.2(syst) \pm 0.3(model)) \cdot 10^{-4}$ for this decay. This result is preliminary.

5 Acknowledgements

We are greatly indebted to our funding agencies for their support in building and operating the Belle detector, and to the KEKB accelerator group for the excellent operation of the KEKB accelerator.

References

1. M. Kobayashi and T. Maskawa, Prog. Theor. Phys. **49**, 652 (1973).
2. M. Battaglia and L. Gibbons, Phys. Rev. D **66** (2002) 010001.
3. Y. Kwon, Proceedings of the XXXIth International Conference on High Energy Physics (ICHEP 2002), 24 - 31 July 2002, Amsterdam, The Netherlands.
4. E. Kikutani ed., KEK Preprint 2001-157 (2001), to appear in Nucl. Instr. and Meth. A.
5. A. Abashian *et al.* (Belle Collab.), Nucl. Instr. and Meth. **A 479**, 117 (2002).
6. N. Isgur and D. Scora, Phys. Rev. D **52**, 2783 (1995). See also N. Isgur *et al.*, Phys. Rev. D **39**, 799 (1989).
7. L. Del. Debbio *et al.*, Phys. Lett. B **416**, 392 (1998).
8. P. Ball and V. M. Braun, Phys. Rev. D **58**, 094016 (1998).
9. K. Hagiwara *et al.*, Phys. Rev. D **66**, 010001 (2002).
10. G. C. Fox and S. Wolfram, Phys. Rev. Lett. **41**, 1581 (1978).
11. R. A. Fisher, Annals of Eugenics **7**, 179 (1936).
12. R. Barlow, C. Beeston, J. Comp. Phys. **72** (1987) 202.

BELLE

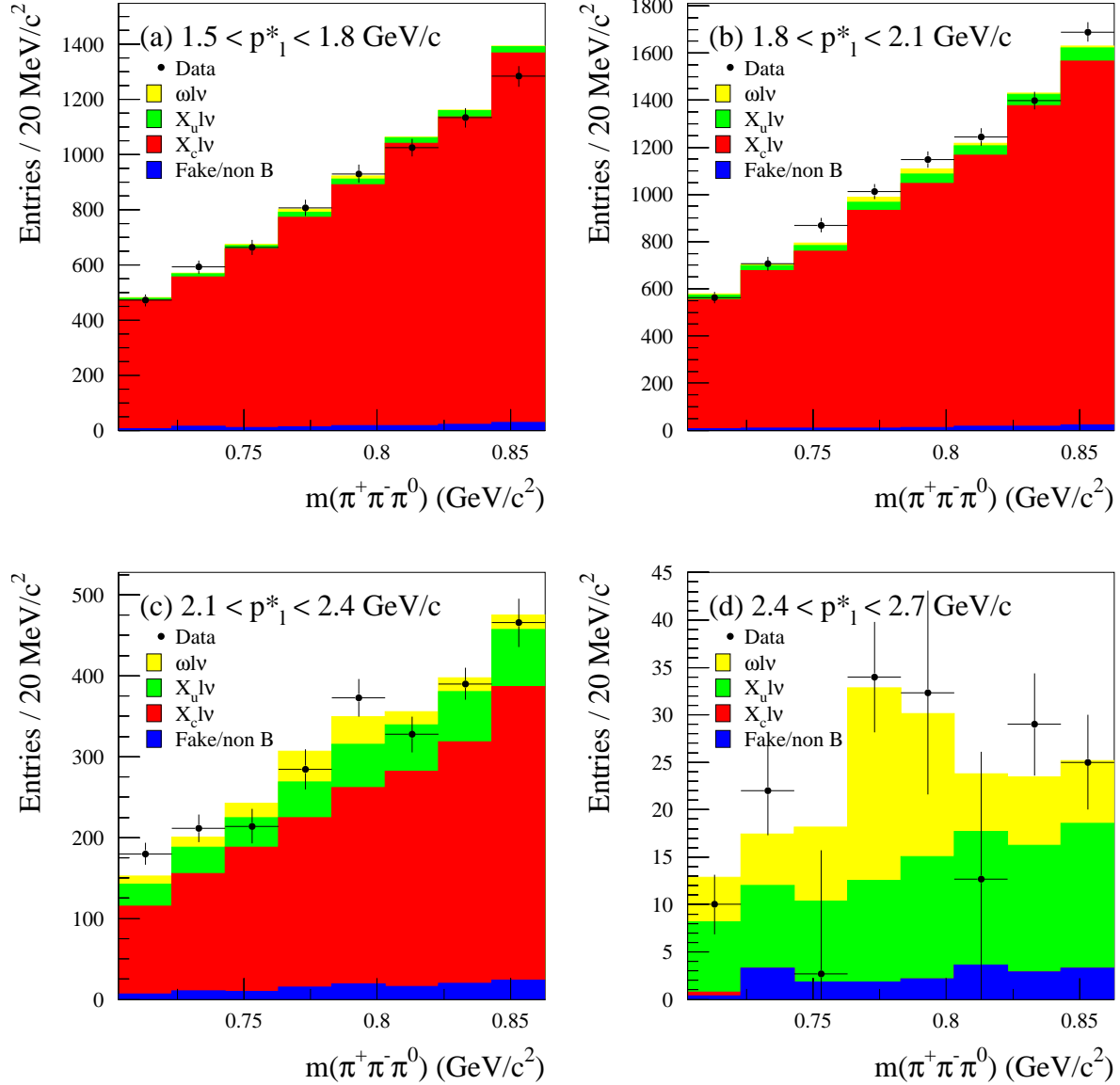


Figure 2. The result of the fit in bins of p_1^* , using ISGW2 form factors for the decay $B^+ \rightarrow \omega l^+ \nu$. The data points are continuum subtracted on-resonance data, the histograms are the components of the fit, as described in the text.

form factor model	$N(B^+ \rightarrow \omega l^+ \nu)$	$\mathcal{B}(B^+ \rightarrow \omega l^+ \nu)$	χ^2
ISGW2	359 ± 106	$(1.02 \pm 0.30) \cdot 10^{-4}$	30.5
UKQCD	428 ± 134	$(1.43 \pm 0.45) \cdot 10^{-4}$	30.6
LCSR	476 ± 156	$(1.73 \pm 0.57) \cdot 10^{-4}$	30.6
average	421 ± 132	$(1.39 \pm 0.44) \cdot 10^{-4}$	

Table 1. The signal yield, the corresponding $B^+ \rightarrow \omega l^+ \nu$ branching fraction and the χ^2 of the fit (ndf = 31), for each of the three form factor models used.